

01

## A model of the propagation of a terahertz pulse through ceramics based on hydroxyapatite

© A.E. Rezvanova,<sup>1</sup> B.S. Kudryashov,<sup>1</sup> D.D. Skorobogatov,<sup>1,2</sup> A.N. Ponomarev<sup>1,2</sup>

<sup>1</sup>Institute of Strength Physics and Materials Science, Siberian Branch, Russian Academy of Sciences, 634055 Tomsk, Russia

<sup>2</sup>Tomsk State University of Control Systems and Radioelectronics, 634050 Tomsk, Russia

e-mail: ranast@ispms.ru, bsk3@ispms.ru, alex@ispms.ru, danilskor1@gmail.com

Received January 29, 2024

Revised January 29, 2024

Accepted January 29, 2024

Computer models of transmission of terahertz (THz) radiation through samples of porous composite ceramics based on hydroxyapatite (HA) with carbon nanotubes (CNTs) additives are developed by using finite element method. The models allowed us to estimate the influence of CNTs additives with 0.1 and 0.5 wt.% concentrations on the structure and optical properties of the samples. Optical properties of the model samples, such as refractive index and absorption coefficient, were determined by using the modeling results of the intensity and transmission rate of THz radiation. It was found, that the increasing of the absorption coefficient and the decreasing of the refractive index are observed with an increase of the porosity of the material, which is due to the denser structure of the material with addition of CNTs. The obtained optical parameters of the HA and HA-CNTs samples models have a qualitative agreement with experimental data and with the literature parameters of bone tissues.

**Keywords:** modeling, finite element method, optical properties, porosity.

DOI: 10.21883/0000000000

### Introduction

The creation of materials for the replacement of bone defects with mechanical properties similar to the bone properties [1–3] is an urgent area of studies of materials science.

Ceramics based on hydroxyapatite (HA) are widely used for creating implants for bone tissue reconstruction due to their structural similarity to the mineral component, high biological activity and biocompatibility with human bone tissue [4,5]. At the same time, the properties of HA ceramics, such as strength, fracture toughness, and porosity, differ significantly from the properties of human bone tissue [6,7], which limits the use in implantation sites with high mechanical loads.

One of the important structural parameters of materials, including ceramic, is the porosity [8], which directly affects the mechanical [3] and optical [9–11] properties, which should be taken into account when developing implants based on such materials.

The porosity of HA-based ceramics can change in case of introduction of various reinforcing additives, such as multi-walled carbon nanotubes (MWCNTs) into the ceramic matrix. MWCNTs additives fill the pore space of the HA [12,13] matrix and increase the density of composites by activating the sintering process in ceramics [1,14]. This results in the strengthening of the grain boundaries of HA ceramics and preserving the microstructure of the matrix, and, as a result, it prevents or slows down the occurrence and spread of cracks in the ceramic composite [15], which

makes it possible to obtain a material with lower porosity compared to HA without additives.

The surface porosity of the HA-based composite decreased from  $10 \pm 1.5$  to  $5 \pm 2.5\%$  with the addition of 4 wt.% MWCNTs additives in Ref. [16]. At the same time, there is a higher porosity in the center of the sample (10%) than in the periphery (5%), which is the result of a compaction gradient. The effect of the functionalization of HA ceramics without and with MWCNTs additives on the mechanical and biological properties of composites was studied in Ref. [17]. The porosity slightly decreases from 2 to 1.5% in nonfunctionalized HA ceramic samples in case of addition of 1 wt.% of MWCNTs. The impact of MWCNTs on the structure and mechanical properties of ceramics  $ZrO_2$  was studied in Ref. [18]. The addition of 0.5 wt.% MWCNTs together with Ni to the  $ZrO_2$  matrix resulted in a decrease of the porosity of the material from 93.8 to 88%. 1.5 wt.% MWCNTs is introduced into ceramics  $Al_2O_3$  in Ref. [19], which resulted in a decrease of porosity from 8 to 4%. Therefore, the use of MWCNTs as reinforcing additives in various matrices contributes to the production of a composite material with a given structure.

One of the methods for studying the porous structure of materials is terahertz (THz) spectroscopy in the time domain Ref. [20–22]. Studying the behavior of the THz pulse makes it possible to study the internal structure of materials and determine their optical properties, such as the absorption coefficient, refractive index and time delay of the THz pulse propagation, used for qualitative analysis of the porosity of materials [23]. The optical properties of

ceramic materials depend on the effects associated with the spatial distribution of local electric fields, and are caused by the scattering of THz radiation by both individual structural elements and their groups [24].

Therefore, the determination of optical properties allows obtaining important information about the internal structure, which shall be taken into account for the analysis of the porosity of materials.

Studies of the optical properties of the material are performed due to the need to obtain a variety of experimental samples with different content of MWCNTs additives, as well as for processing a large amount of experimental data.

To optimize the research task, it makes sense to use computer modeling methods, among which the finite element method (FEM) is the most preferred. This method has proven itself in the field of engineering and mathematical modeling in the problems of structural analysis, heat transfer, fluid flow, mass transfer and electromagnetic potential [25].

For instance, FEM was used in Ref. [26] to simulate the electrical conductivity of two-dimensional and three-dimensional media in the presence of ideally conductive or insulating inclusions. Another example of usage of FEM is the modeling of core-shell nanoparticles that combine strain-coupled magnetostrictive and piezoelectric phases, and their magnetoelectric behavior is analyzed [27].

This work is aimed at developing simulation models of THz radiation transmission through the porous structure of HA-based materials with the addition of 0.1 and 0.5 wt.% MWCNTs.

## 1. Research methods

### 1.1. Modeling of the structure

Computer programs are used for conducting computational experiment to simulate the studied objects and the processes occurring with them, as well as to obtain arrays of output calculated values [28–30]. COMSOL Multiphysics [30] modeling environment based on the finite element method (FEM) is used to address the problem raised in this paper.

A program was created in this environment for the automatic construction of structural models of a composite material based on specified parameters, such as sample size, number of pores, maximum and minimum pore radii, minimum and maximum number of CNTs in pores.

An algorithm for creating models of the porous structure of materials with inclusions in the form of nanotubes:

1) creation of the basis of the model in the form of a cylinder with a radius of  $20\ \mu\text{m}$  and a height of  $40\ \mu\text{m}$ ;

2) formation of balls with a radius from 0.1 to  $1\ \mu\text{m}$  and cutting them out of the main cylinder using the Difference tool to form pores;

3) creation of a cylinder with a radius of 9 nm and a height of  $15\ \mu\text{m}$  in a random direction in each formed pore for modeling of CNTs;

4) adding similar-sized cylinders with different angles of inclination to each cylinder created in the pore to form CNTs agglomerates;

5) the formation of an outer layer of HA around the CNTs with a radius of  $45\ \mu\text{m}$  and a height equal to the height of the CNT;

6) creation of additional cylinders equal to the main one in size for trimming each CNT from the surface of the model using the Intersection tool.

Composite material models based on a simplified representation of the MWCNTs in the form of a solid cylinder are proposed in this study. The key parameter of these models is the diameter of the cylinder, equal to 18 nm, which corresponds to the experimentally determined diameter of the MWCNTs.

The stages of creation of a model of the structure of a composite material based on HA with the addition of CNTs are graphically shown in Fig. 1.

### 1.2. Modeling of the transmission of THz radiation

FEM embedded in the COMSOL Multiphysics [31] environment was used to calculate the optical properties of the models, such as the refractive index and absorption coefficient. Release from Grid module was used to build a computer model of terahertz (THz) radiation transmission by specifying a network of points for radiation sources. A cylindrical type grid was built using this module in which the starting points for the rays are on a circle, and the rays themselves are directed perpendicular to a given plane. Two grids were built to analyze the effect of the radiation propagation area on the optical properties of the model (Fig. 2).

The beam is divided into reflected and refracted (Fig. 3) in the calculation of the trajectory of motion when the beam reaches the interface between two media with different refractive indices and the direction of movement of both beams is calculated according to the Snellius law (1):

$$n_1\theta_1 = n_2\theta_2, \quad (1)$$

where  $n_1$  — the refractive index of the medium from which light falls on the interface,  $\theta_1$  — the angle between the ray incident on the surface and the normal to the surface,  $n_2$  — the refractive index of the medium into which the light falls after passing the interface,  $\theta_2$  — the angle between the beam passing through the surface and the normal to the surface.

A plane wave with a given frequency of 1 THz was selected to simulate the passage of rays. The initial radiation intensity was  $1000\ \text{W/m}^2$ . The radiation frequency was determined based on an experiment conducted in the frequency range from 0.25 to 1.3 THz [32]. Due to the fact that the measurement error increased when approaching the boundary values, it was decided to use the average frequency value. In addition, the choice of the radiation

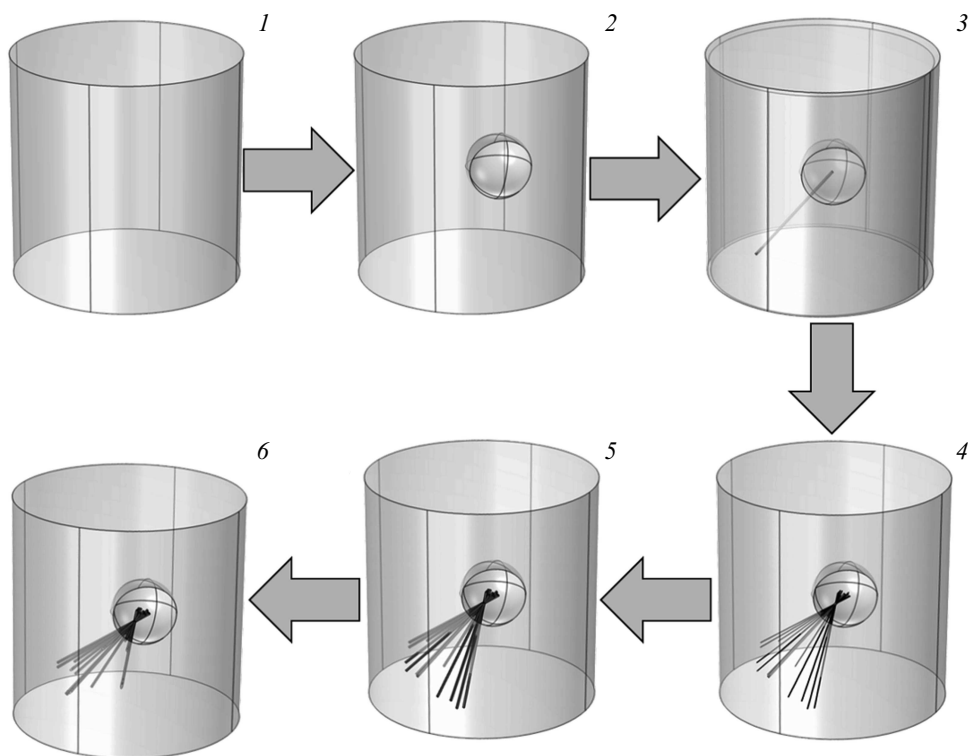


**Figure 1.** Stages of creation of a model of the porous structure of a cylindrical sample: 1 — creation of a cylindrical base, 2 — pore formation, 3 — creation of an axial CNTs, 4 — addition of the remaining CNTs, 5 — addition of an outer layer of HA around the nanotubes, 6 — trimming of the nanotubes at the boundary with the surface.

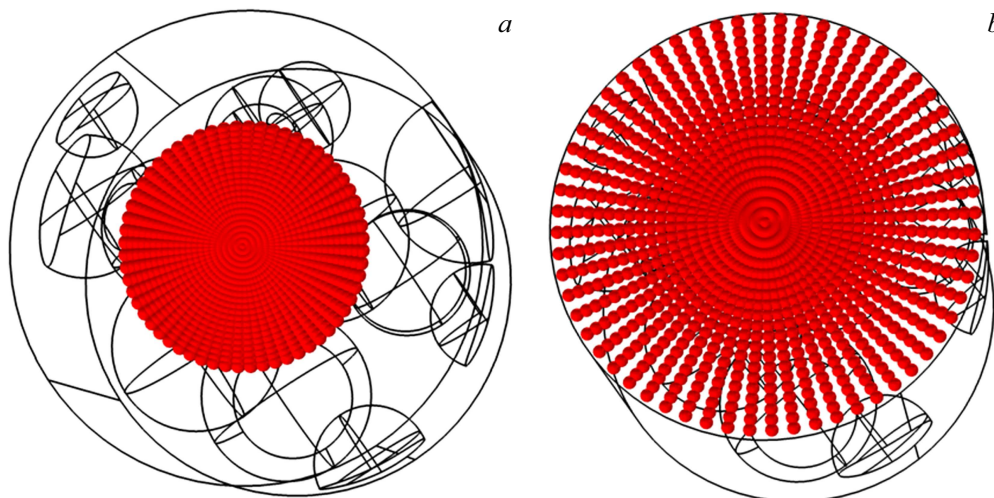


**Figure 2.** Radiation sources in a cylindrical sample: the passage of radiation through the center of the radial section (a), through the entire surface of the radial section (b).

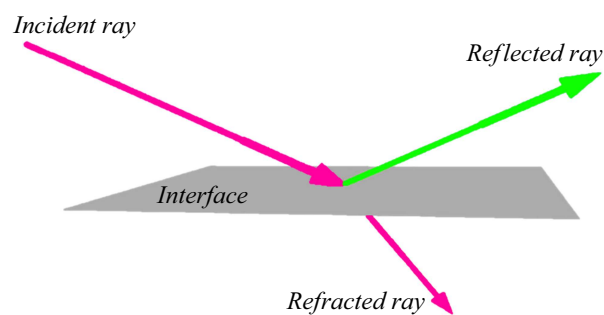


**Figure 3.** The separation of the beam into reflected and refracted at the boundary of the media [31].

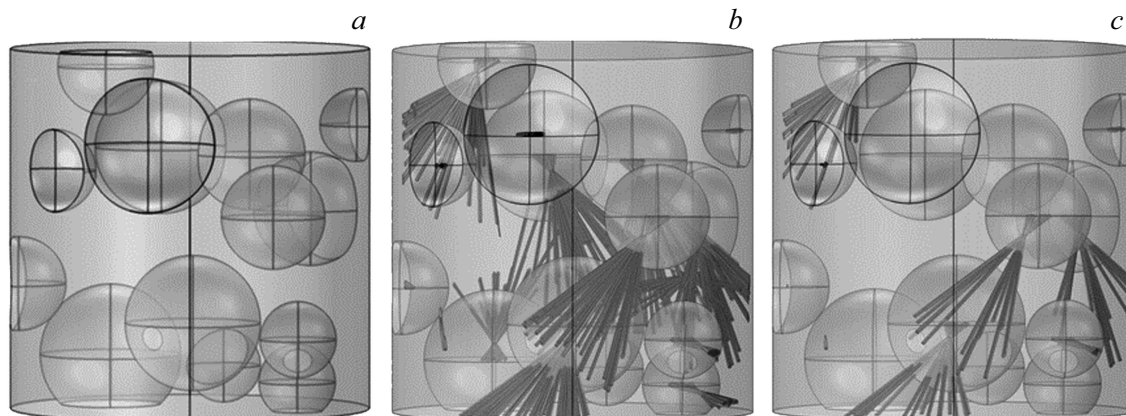


**Figure 4.** Models of structures of ceramic samples based on HA of three types: *a* —HA, *b* —HA-0.1 wt.% CNTs, *c* —HA-0.5 wt.% CNTs.

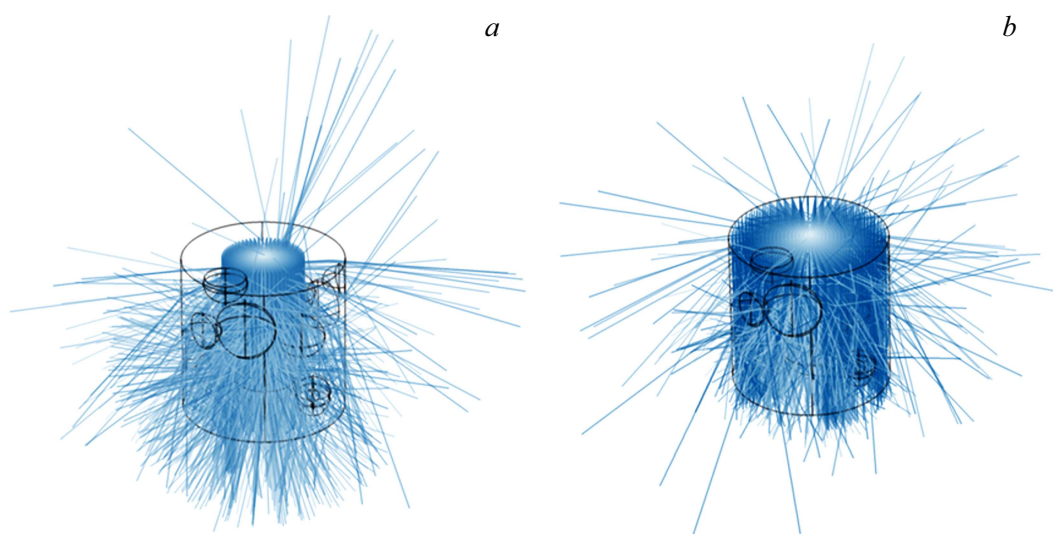


**Figure 5.** Models of THz radiation transmission for a HA sample without additives: *a* — through the center of the radial section, *b* — through the entire surface of the radial section.

frequency in the simulation is due to the presence of a maximum absorption peak at a frequency of  $\sim 1$  THz, the explanation of which is presented in Ref. [32].

## 2. Modeling of optical properties of ceramic samples based on hydroxyapatite

Figure 4 shows models of porous structures of ceramic samples based on HA of three types: without CNT additives, with the addition of 0.1 and 0.5 wt.% CNT.

The transmission of THz radiation through these structures was modeled in two ways: through the center and the entire surface of the radial section of the model. Fig. 5 shows the result of radiation transmission for HA without additives, Fig. 6 shows the result of radiation transmission for HA with added 0.1 and 0.5 wt.% CNTs.

The radiation intensity for each model was calculated using The Ray Optics Module [31]. The absorption coefficients were calculated based on the data obtained using the Booger-Lambert-Baer law (2):

$$I(l) = I_0 e^{-k_\lambda l}, \quad (2)$$

where  $I(l)$  — output intensity,  $[W/m^2]$ ,  $I_0$  — intensity input signal,  $[W/m^2]$ ,  $k_\lambda$  — absorption coefficient,  $[cm^{-1}]$ ,  $l$  — material thickness,  $[mm]$ .

Figure 7 shows the dependences of intensities and absorption coefficients on the porosity of models of samples with different CNT content in the HA matrix (1 —HA without additives, 2 —HA-0.1 wt.% CNTs, 3 — HA-0.5 wt.% CNTs). Porosity  $P$  was determined as the ratio of the volume of formed pores to the total volume of the material [8] according to the formula (3):

$$P = \left( \frac{V_p}{V_0} \right) \cdot 100\%, \quad (3)$$



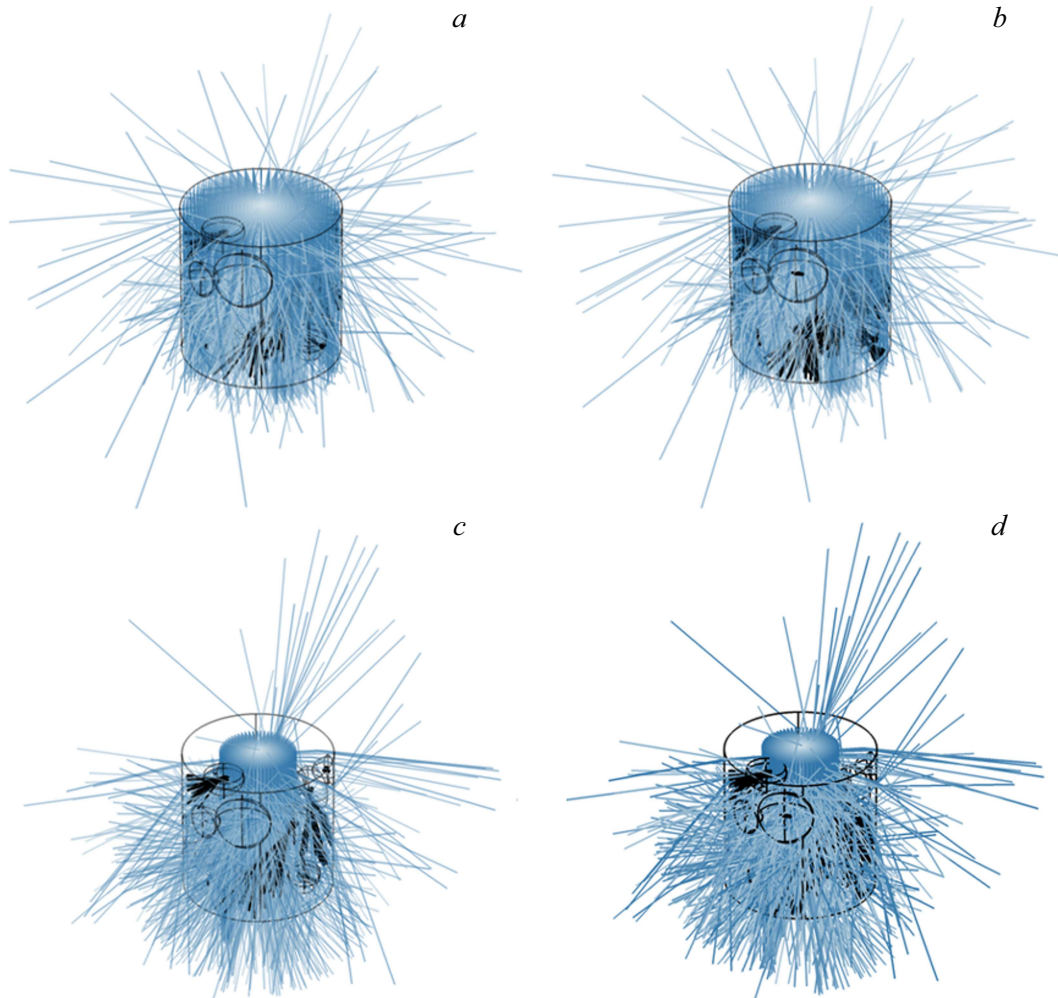


**Figure 6.** Transmission of THz radiation for models of HA-0.1 wt.% CNTs: *a* — through the center of the radial section, *c* — through the entire surface of the radial section; HA-0.5 wt.% CNTs: *b* — through the center of the radial section, *d* — through the entire surface of the radial section.

where  $V_p$  — the volume of pores in the material,  $V_0$  — the volume of the main cylinder.

It is shown that a decrease of the intensity of the passage of the THz beam and an increase of the absorption coefficient are observed with an increase of the porosity of the material.

Next, the absolute refractive index was calculated using the formula (4):

$$n = \frac{c}{v_{\text{sample}}}, \quad (4)$$

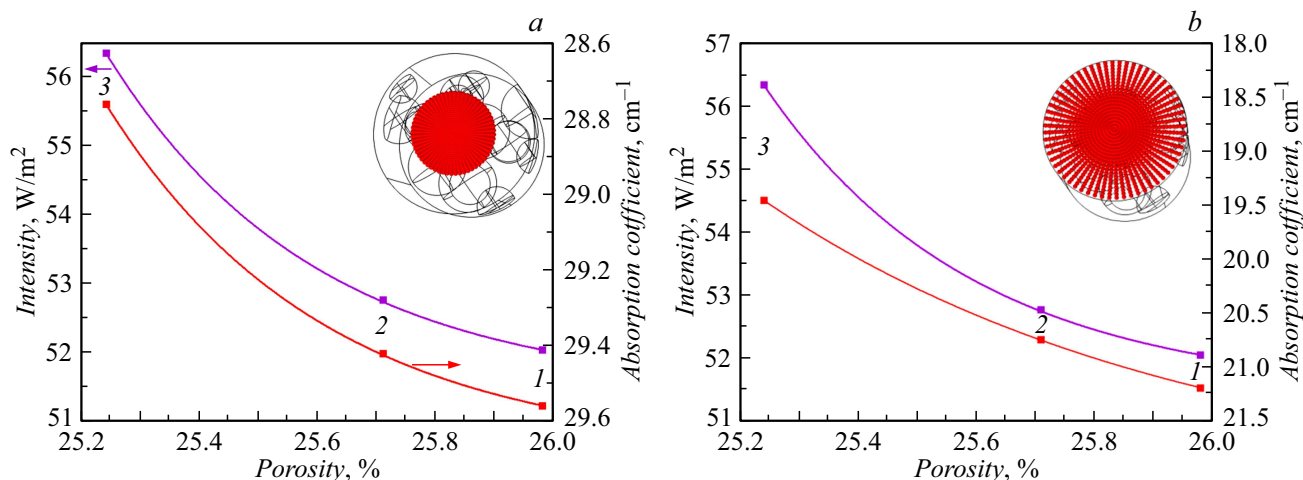
where  $n$  — refractive index,  $c$  — the speed of light in vacuum, m/s,  $v_{\text{sample}}$  — the speed of radiation propagation in matter, m/s [33].

Figure 8 shows the dependence of the refractive index on the porosity of the models (1 — HA, 2 — HA-0.1 wt.% CNTs, 3 — HA-0.5 wt.% CNTs). It can be seen that the refractive index decreases with the increase of porosity. The generalized results of the optical properties of the models are summarized in Table 1.

The obtained data for modeling porosity and optical properties were compared with the results of an experimental study of HA-MWCNTs composite ceramics by THz spectroscopy in the time domain in the frequency range from 0.2 to 1.3 THz [32] (Table 2). The porosity of the samples was experimentally determined by the Archimedes method using a theoretical density of  $3.167 \text{ g/cm}^3$  for stoichiometric HA and varied from 8 to 27.5% with an increase of the content of MWCNTs additives to 0.5 wt.%. A detailed description of the technique for producing composite ceramics is provided in Ref. [1].

A comparison of the results of modeling the absorption and refraction of HA-CNTs composites showed quantitative agreement with the literature data on the optical properties of HA and human bone tissues, in particular, with cortical and trabecular bones [36–38] (Table 3).

The adequacy of the obtained models is confirmed by qualitative agreement with the parameters obtained during the experiment on studying the porous structure of HA-MWCNTs ceramics by THz spectroscopy [32]. The model



**Figure 7.** Dependences of intensities and absorption coefficients on the porosity of the models: *a* — through the center of the radial section, *b* — through the entire surface of the radial section.

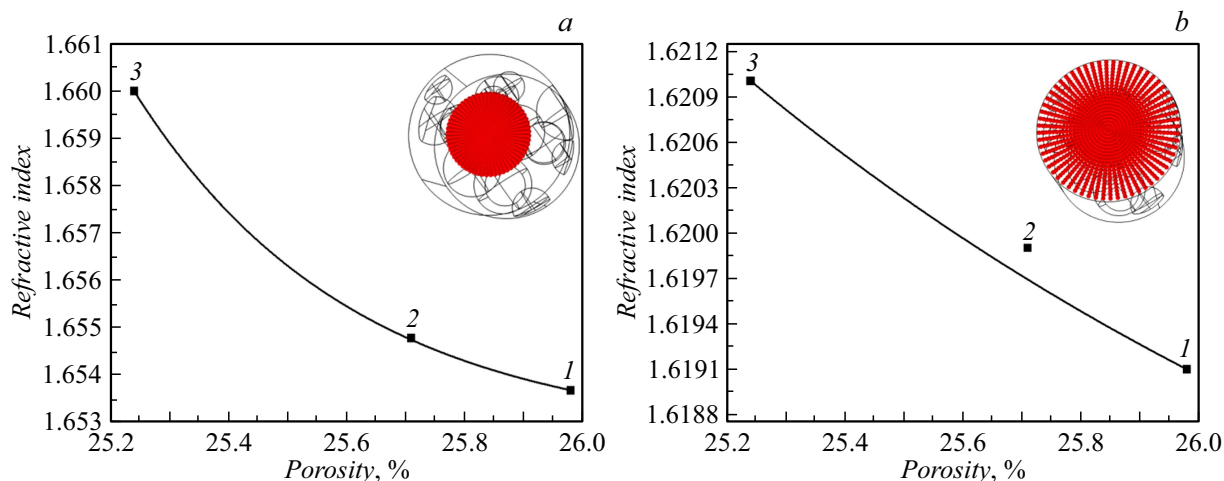


**Figure 8.** Dependences of refractive indices on the porosity of models: *a* — through the center of the radial section, *b* — through the entire surface of the radial section.

**Table 1.** Results of modeling optical properties

Transmission of a THz radiation beam through the center of the radial section of the model				
CNTs, wt. %	Porosity, %	Intensity, W/m <sup>2</sup>	Indicator index	Coefficient Absorption, cm <sup>-1</sup>
0.0	25.98	52.05	1.654	29.56
0.1	25.71	52.77	1.655	29.42
0.5	25.24	56.34	1.660	28.76
Transmission of the THz radiation beam through the entire surface of the radial section of the model				
0.0	25.98	52.05	1.6191	21.19
0.1	25.71	52.77	1.6199	20.75
0.5	25.24	56.34	1.6210	19.45

**Table 2.** Experimental data on the optical properties of HA ceramics [32]

Experimental data of THz spectroscopy			
MWCNTs, wt.%	Porosity, %	Indicator index	Coefficient Absorption, $\text{cm}^{-1}$
0.0	27.5	2.54	34.69
0.1	23	2.70	28.5
0.5	8	2.83	27.6

**Table 3.** Literature data on optical properties of materials

Material	Indicator index	Coefficient Absorption, $\text{cm}^{-1}$
HA	1.64 [34]	37.08 [35]
Cortical bone	1.94 [36]	43.42 [36]
	2.34 [37]	56.54 [37]
Trabecular Bone	0.97 [38]	19.6 [38]
Enamel	2.91 [39]	43.33 [40]
Dentin	2.41 [39]	48.76 [40]

with transmission of radiation through the center of the radial section of the sample is the closest to the experimental method for studying optical properties.

## Conclusion

A program was developed for the automated creation of a porous structure of samples based on HA with the addition of various concentrations of CNTs. Structural models of three types are built using this program: HA ceramics without additives and composites HA-0.1 wt.% CNTs, HA-0.5 wt.% CNTs, through which the THz radiation transmission process was modeled using the finite element method, which allows us to evaluate the effect of CNTs additives on the structure and optical properties of samples. Two types of passage of THz radiation through the center and the entire surface of the radial section of the models are modeled and the models with transmission of radiation through the center of the sample section have the greatest similarity with the experiment among these models. The absorption coefficients were calculated in accordance with the Beer-Lambert-Baer law for each model using the values of the transmission intensities of THz radiation, as well as absolute refractive indices. Based on the results of calculations, a correlation was established between the optical parameters and the porosity of models of ceramic samples based on HA. It was shown that the structure and optical parameters of ceramics can be influenced by changing the porosity by varying the concentrations of CNTs additives. The porosity decreases in both test samples and in obtained models with the introduction of CNTs additives,

which, occupying the pore space of the HA matrix form a denser material.

The developed computer models will reduce time and production costs, both for the synthesis of real samples and for conducting research by supplementing experimental data with simulation results.

## Funding

The paper was prepared as part of the state assignment of the Institute of Strength Physics and Materials Science of the Siberian Branch of the Russian Academy of Science, subject № FWRW-2022-0002.

## Conflict of interest

The authors declare that they have no conflict of interest.

## References

- [1] M.S. Barabashko, M.V. Tkachenko, A.A. Neiman, A.N. Ponomarev, A.E. Rezvanova. *Appl. Nanosci.*, **10**, 2601 (2020). DOI: 10.1007/s13204-019-01019-z
- [2] R.G. Ribas, V.M. Schatkoski, T.L. do Amaral Montanheiro, B.R.C. deMenezes, C. Stegemann, D.M.G. Leite, G.P. Thim. *Ceram. Intern.*, **45**(17), 21051 (2019). DOI: 10.1016/j.ceramint.2019.07.096
- [3] Y. Han, Q. Wei, P. Chang, K. Hu, O.V. Okoro, A. Shavandi, L. Nie. *Crystals*, **11**(4), 353 (2021). DOI: 10.3390/cryst11040353
- [4] T. Zhang, W. Cai, F. Chu, F. Zhou, S. Liang, C. Ma, Y. Hu. *Compos. Part A Appl. Sci. Manuf.*, **128**, 105681 (2020). DOI: 10.1016/j.compositesa.2019.105681
- [5] E. Fiume, G. Magnaterra, A. Rahdar, E. Vern., F. Bairo. *Ceramics*, **4**(4), 542 (2021). DOI: 10.3390/ceramics4040039
- [6] X. Zhao, J. Zheng, W. Zhang, X. Chen, Z. Gui. *Ceram. Intern.*, **46**(6), 7903 (2020). DOI: 10.1016/j.ceramint.2019.12.010
- [7] P. Khalid, V.B. Suman. *J. Bionanosci.*, **11**(3), 233 (2017). DOI: 10.1166/jbns.2017.1431
- [8] P. Greg, K. Sing. *Adsorbciya, udel'naya poverhnost', poristost'* (Mir, M., 1984) (in Russian).
- [9] O.J. Akinribide, G.N. Mekgwe, S.O. Akinwamide, F. Gamaoun, C. Abeykoon, O.T. Johnson, P.A. Olubambi. *J. Mater. Res. Tech.*, **21**, 712 (2022). DOI: 10.1016/j.jmrt.2022.09.027
- [10] A. Wagner, B. Ratzker, S. Kalabukhov, M. Sokol, N. Frage. *J. Eur. Cer. Soc.*, **39**(4), 1436 (2019). DOI: 10.1016/j.jeurceramsoc.2018.11.006

- [11] R. Shahmiri, O.C. Standard, J.N. Hart, C.C. Sorrell. *J. Prosthet. Dent.*, **119** (1), 36 (2018). DOI: 10.1016/j.prosdent.2017.07.009
- [12] F. Moussy. *J. Biomed. Mat. Res. A*, **94** (4), 1001 (2010). DOI: 10.1002/jbma.a.32866
- [13] A. Faingold, S.R. Cohen, R. Shahar, S. Weiner, L. Rapoport, H.D. Wagner. *J. Biomech.*, **47** (2), 367 (2014). DOI: 10.1016/j.jbiomech.2013.11.022
- [14] M.S. Barabashko, M.V. Tkachenko, A.E. Rezvanova, A.N. Ponomarev. *Russ. J. Phys. Chem.*, **95** (5), 1017 (2021). DOI: 10.1134/S0036024421050058
- [15] D. Veljović, G.D. Vuković, I. Steins, E. Palcevskis, P. Uskoković, R. Petrović, D. Janačković. *Sci. Sinter.*, **45** (2), 33 (2013). DOI: 10.2298/SOS1302233V
- [16] D. Lahiri, V. Singh, A.K. Keshri, S. Seal, A. Agarwal. *Carbon*, **48** (11), 3103 (2010). DOI: 10.1016/j.carbon.2010.04.047
- [17] S. Mukherjee, B. Kundu, A. Chanda, S. Sen. *Ceram. Int.*, **41** (3), 3766 (2015). DOI: 10.1016/j.ceramint.2014.11.052
- [18] B. Henriques, D. Fabris, E. Lopes, A.C. Moreira, I.F. Mantovani, C.P. Fernandes, M.C. Fredel. *Adv. Eng. Mater.*, **24** (1), 2100624 (2022). DOI: 10.1002/adem.202100624
- [19] L. Yu, P. Jia, Y. Song, B. Zhao, Y. Pan, J. Wang, H. Cui, R. Feng, H. Li, X. Cui, Z. Gao, X. Fang, L. Zhang. *J. Mater. Res. Tech.*, **18**, 3541 (2022). DOI: 10.1016/j.jmrt.2022.04.035
- [20] A.S. Nikoghosyan, H. Ting, J. Shen, R.M. Martirosyan, M.Yu. Tunyan, A.V. Papikyan, A.A. Papikyan. *J. Contemp. Phys. Arme.*, **51**, 56 (2016). DOI: 10.3103/S1068337216030087
- [21] P. Bawuah, T. Ervasti, N. Tan, J.A. Zeitler, J. Ketolainen, K.-E. Peiponen. *Int. J. Pharm.*, **509** (1-2), 439 (2016). DOI: 10.1016/j.ijpharm.2016.06.023
- [22] Yu.V. Kistenev, V.V. Nikolaev, O.S. Kurochkina, A.V. Borisov, E.A. Sandykova, N.A. Krivova, D.K. Tuchina, P.A. Timoshina. *Opt. Spectr.*, **126**, 523 (2019). DOI: 10.1134/S0030400X19050138
- [23] P. Bawuah, D. Markl, D. Farrell, M. Evans, A. Portieri, A. Anderson, D. Goodwin, R. Lucas, J.A. Zeitler. *J. Inf. Millim. Te. W.*, **41**, 450 (2020). DOI: 10.1007/s10762-019-006590
- [24] D.S. Bezmelnitsin, D.A. Lizunkova, I.A. Shishkin. *Vestnik molodyh uchenykh i specialistov Samarskogo un-ta*, **1** (16), 261 (2020) (in Russian).
- [25] J. Fish, T. Belytschko. *A First Course in Finite Elements* (John Wiley & Sons, 313, 2007)
- [26] P.E. Sizin. *Mining information and analytical bulletin*, **5**, 43 (2023) (in Russian).
- [27] S. Fiochi, E. Chiaramello, A. Marrella, G. Suarato, M. Bonato, M. Parazzini, P. Ravazzani. *PloS one*, **17** (9), E0274676 (2022). DOI: 10.1371/journal.pone.0274676
- [28] V.V. Dmitriev, T.V. Gandzha, I.M. Dolganov, N.V. Aksenova. *Pet. Coal.*, **59** (4), 429 (2017).
- [29] T.V. Gandzha, K.A. Isakov, A.V. Shapovalov. *Russ. Phys. J.*, **65** (4), 663 (2022). DOI: 10.1007/s11182-022-02682-6
- [30] COMSOL [Electronic resource] Available at: <https://www.comsol.ru/>. Date of access: 28.11.2023
- [31] Ray Optics Module User's Guide [Electronic resource] <https://doc.comsol.com/5.4/doc/com.comsol.help.roptics/RayOpticsModuleUsersGuide.pdf>. Date of access: 28.11.2023
- [32] A.E. Rezvanova, B.S. Kudryashov, A.N. Ponomarev, A.I. Knyazkova, V.V. Nikolaev, Y.V. Kistenev. *Nanosystems: Phys. Chem. Math.*, **14** (5), 530 (2023). DOI: 10.17586/2220-8054-2023-14-5-530-538
- [33] S.I. Borisenko, O.G. Revinskaya, N.S. Kravchenko, A.V. Chernov. *Pokazatel' prelomleniya sveta i metody ego eksperimental'nogo opredeleniya* (Izd-vo Tomskogo politekh. un-ta, Tomsk, 2014) (in Russian).
- [34] P. Huang, B. Zhou, Q. Zheng, Y. Tian, M. Wang, L. Wang, J. Li, W. Jiang. *Adv. Mater.*, **32** (1), 905951 (2020). DOI: 10.1002/adma.201905951
- [35] M. Plazanet, J. Tasseva, P. Bartolini, A. Taschin, R. Torre, C. Combes, C. Rey, A. Di Michele, M. Verezhak, A. Gourrier. *PLoS One*, **13** (8), E0201745 (2018). DOI: 10.1371/journal.pone.0201745
- [36] M. Bessou, B. Chassagne, J.-P. Caumes, C. Pradere, P. Maire, M. Tondusson, E. Abraham. *Appl. Opt.*, **51** (28), 6738 (2012). DOI: 10.1364/AO.51.006738
- [37] M.R. Stringer, D.N. Lund, A.P. Foulds, A. Uddin, E. Berry, R.E. Miles, A.G. Davies. *Phys. Med. Biol.*, **50** (14), 3211 (2005). DOI: 10.1088/0031-9155/50/14/001
- [38] A.S. Nikoghosyan, J. Shen, H. Ting. *Physical Properties of Human Jawbone, Spongy Bone, Collagen and Cerabone Bone Transplantation Material in Range of 0.2 to 2.5 THz*, 44th Intern. Conf. on Infrared, Millimeter, and Terahertz Waves, IRMMW-THz, IEEE, **1–2**, (2019). DOI: 10.1109/IRMMW-THz.2019.8873754
- [39] J. Cai, M. Guang, J. Zhou, Y. Qu, H. Xu, Y. Sun, H. Xiong, S. Liu, X. Chen, J. Jin, X. Wu. *Opt. Express*, **30** (8), 13134 (2022). DOI: 10.1364/OE.452769
- [40] Y.C. Sim, I. Maeng, J.-H. Son. *Curr. Appl. Phys.*, **9** (5), 946 (2009). DOI: 10.1016/j.cap.2008.09.008

Translated by A.Akhtyamov